Embryonic and Neonatal Phenotyping of Genetically Engineered Mice

Shathiyah Kulandavelu, Dawei Qu, Nana Sunn, Junwu Mu, Monique Y. Rennie, Kathie J. Whiteley, Johnathon R. Walls, Nicholas A. Bock, John C. H. Sun, Andrea Covelli, John G. Sled, and S. Lee Adamson

Abstract

Considerable progress has been made in adapting existing and developing new technologies to enable increasingly detailed phenotypic information to be obtained in embryonic and newborn mice. Sophisticated methods for imaging mouse embryos and newborns are available and include ultrasound and magnetic resonance imaging (MRI) for in vivo imaging, and MRI, vascular corrosion casts, microcomputed tomography, and optical projection tomography (OPT) for postmortem imaging. In addition, Doppler and M-mode ultrasound are useful noninvasive tools to monitor cardiac and vascular hemodynamics in vivo in embryos and newborns. The developmental stage of the animals being phenotyped is an important consideration when selecting the appropriate technique for anesthesia or euthanasia and for labeling animals in longitudinal studies. Study design also needs to control for possible differences between inter- and intralitter variability, and for possible long-term developmental effects caused by anesthesia and/or procedures. Noninvasive or minimally invasive intravenous or intracardiac injections or blood sampling, and arterial pressure and electrocardiography (ECG) measurements are feasible in newborns. Whereas microinjection techniques are available for embryos as young as 6.5 days of gestation, further advances are required to enable minimally invasive fluid or tissue samples, or blood pressure or ECG measurements, to be obtained from mouse embryos in utero. The growing repertoire of techniques available for phenotyping mouse embryos and newborns promises to accelerate knowledge gained from studies using genetically engineered mice to understand molecular regulation of morphogenesis and the etiology of congenital diseases.

Key Words: anesthesia; corrosion casting; embryo; magnetic resonance imaging; microinjections; phenotype; tomography; ultrasonography

Genetic mouse models have yielded remarkable insights into the gene products that control morphological development in the embryo (Bruneau 2003; Conway et al. 2003; Copp 1995), and valuable new models of human congenital diseases have been developed (e.g., Bruneau 2003). When exploring the function of genes that cause congenital diseases and/or embryonic or neonatal lethality, it is necessary to evaluate the phenotype in the critical developmental period. Clearly, the major challenge when phenotyping mouse embryos is their small size (Figure 1); embryos weigh $\leq$1 g throughout most of gestation (Figure 2). Nevertheless, we have documented that detailed phenotypic information can be obtained from embryos and/or neonates using both noninvasive in vivo and acute invasive approaches.

In this article, we describe a variety of in vivo and acute invasive methods for phenotyping embryonic and newborn mice. Remarkable advances in imaging technology are enabling images of increasingly high resolution to be obtained

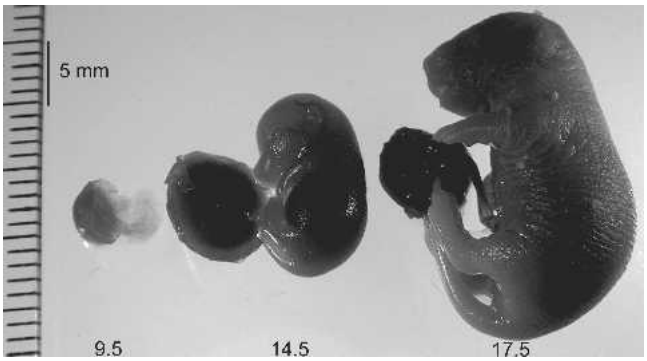

Figure 1 Images of embryos and placentas obtained using a light microscope at gestational days 9.5, 14.5, and 17.5. The embryo at day 9.5 of gestation is nearly transparent. The scale bar is in mm.

Shathiyah Kulandavelu, B.Sc. (Hons), Dawei Qu, M.D., Ph.D., Nana Sunn, Ph.D., Junwu Mu, M.D., Ph.D., Kathie J. Whiteley, M.Sc., John C.H. Sun, B.Sc. (Hons), and Andrea Covelli, B.Sc. (Hons), are Graduate Student (S.K.), Senior Technician (D.Q.), Post Doctoral Research Fellows (N.S. and J.M.), Senior Technician (K.J.W.), Graduate Student (J.C.H.S.), and Summer Student (A.C.), respectively, at the Samuel Lunenfeld Research Institute, Mount Sinai Hospital, Toronto, Ontario, Canada (SLRI). Ms. Kulandavelu and Mr. Sun are also Graduate Students in the Department of Physiology, University of Toronto, Toronto, Ontario (UT). Monique Y. Rennie, B.Sc., Johnathon R.Walls, M.Sc., Nicholas A. Bock, Ph.D. are or were Graduate Students, and John G. Sled, Ph.D., is Assistant Professor in the Department of Medical Biophysics, UT and the Mouse Imaging Center, Hospital for Sick Children. S. Lee Adamson, Ph.D., is Principal Investigator at SLRI and Professor in the Departments of Obstetrics and Gynecology and of Physiology, UT.

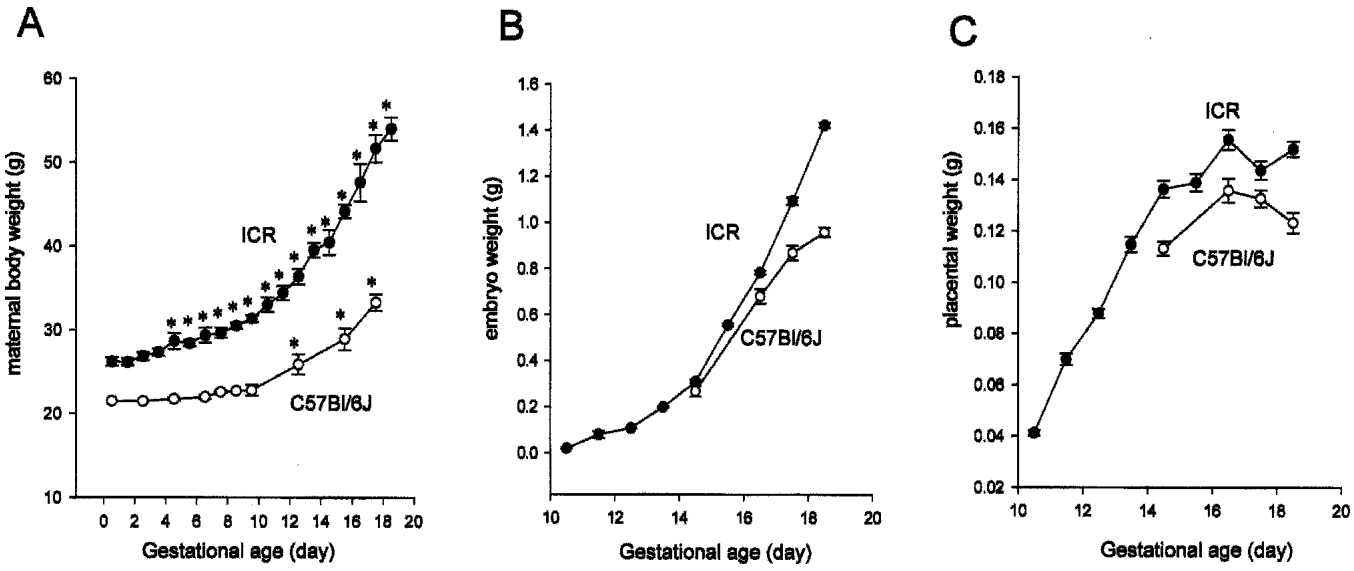

Figure 2 Body and placental weights as a function of gestational age in two strains of mice: ICR (solid circles) and C57Bl/6J (open circles). (A) Maternal body weight increases progressively after mating in both strains although the body weight of ICR females is always greater than C57Bl/6J females. The increase in maternal body weight was significant by 4.5 days of gestation in ICR mice (N = 6-16) but did not reach significance until 12.5 days in C57Bl/6J mice (N = 5-9). * $p < 0.05$. (B) Embryo weight increases exponentially during gestation in ICR mice to reach almost 1.5 g by term. Although body weights of embryos in both strains are similar at mid-gestation, the growth rate of C57Bl/6J embryos slows in late gestation so that at term the body weight of C57Bl/6J embryos (~1 g) is less than that of ICR embryos (~1.5 g). (C) Placental weight gain slows markedly in late gestation in both strains of mice. Placental weight is greater in ICR than C57Bl/6J mice. Data expressed as mean ± standard error.

from embryonic and newborn mice. High-resolution ultrasound imaging of embryos and newborns has proven valuable as a phenotyping tool, and sophisticated new magnetic resonance imaging (MRI[1]) and microcomputed tomography (micro-CT[1]) technologies are generating remarkably detailed images of mice in this age group. We also describe the application of an existing technology, vascular corrosion casting, and an exciting new technology, optical projection tomography (OPT[1]), as phenotyping tools for mouse embryos and newborns. The applications and special features of these imaging modalities are compared in Table 1. Invasive methods that permit direct visualization of the mouse embryo using light microscopic techniques have also been used. Confocal microscopy has been used to image key events in early embryonic development, including embryonic turning and closure of the neural tube (Jones et al. 2002), and to quantify blood velocity in the developing vasculature of the yolk sac in whole mouse embryos in culture (Jones et al. 2004). Intravital videomicroscopy has been used to image the beating heart after surgical exposure of the embryo (Keller et al. 1996).

Most imaging techniques require animals to be immobilized using anesthesia or euthanasia, so we begin by discussing these topics with special reference to pregnant and newborn mice. This section is followed by a brief discussion of the special experimental and statistical considerations that pertain to studies of this age group. Methods for accessing the vasculature for blood collection or injection, and for evaluating cardiovascular function using electrocardiography (ECG[1]), blood pressure, and Doppler blood velocity in newborn and/or embryonic mice, are also described.

Anesthesia of Pregnant and Newborn Mice

Anesthetic agents are frequently used to immobilize mice to reduce motion artifacts during image acquisition or other procedures. Isoflurane, an inhalation anesthetic that is relatively safe when used at appropriate concentrations for both the mice and the human operators (Stimpfel and Gershey 1991), and pentobarbital or ketamine and xylazine given by intraperitoneal injection, are effective in pregnant mice (Furukawa et al. 1998). The advantages of inhalation anesthesia in pregnant and newborn mice include elimination of the risk of intrauterine trauma associated with injectables, similar and readily adjustable dosage regardless of animal age or size, control of the duration of anesthesia, and rapid induction and postanesthetic recovery. In newborns (within a few days of birth), hypothermia is also an effective method of short- and long-term anesthesia (Danneman and Mandrell

[1]Abbreviations used in this article: 2D, two-dimensional; 3D, three-dimensional; CT, computed tomography; ECG, electrocardiography; micro-CT, microcomputed tomography; MRI, magnetic resonance imaging; OPT, optical projection tomography; SEM, scanning electron microscope; UBM, ultrasound biomicroscope.

Table 1 Characteristics of small animal imaging systems suitable for embryonic and newborn mice[a]

	1) Invasiveness 2) Acquisition/ Analysis Time	Applications	Resolution	Specimen Dimensions	Size and Portability	Price (USD)	Safety Concerns	Strengths	Limitations	References (See Text)
MRI	1) In vivo and postmortem 2) Acquisition: 30-180 min Analysis: 5-10 min	Overall anatomical imaging	25-100μm	Unlimited in mice	Room size, requires a special site, stationary	> 1 million	Strong magnetic field	3D, diverse contrast mechanisms (tissue density, water composition and compartmentalization, fluid velocity, and available contrast agents)	Motion artifacts	Chatham and Blackband 2001 Nieman et al. 2005.
Vascular Corrosion Casting and SEM	1) Postmortem 2) Acquisition: 1-2 days Analysis: 120 min	Vascular anatomy of embryo, placenta and newborn (including organs)	< 1 μm	Unlimited for embryonic and neonatal mice	Portable tabletop surgical microscope and stationary SEM	~350,000	Avoid skin contact with casting compound and inhaling vapours	3D, simple and inexpensive	Sample preparation time, limited quantitative analysis	Adamson et al. 2002 Kondo 1998 Whiteley et al. 2006.
Micro-CT	1) In vivo and postmortem 2) Acquisition: 120 min Analysis: 30-60 min	Skeleton, vascular anatomy of embryo, placenta and newborn organs	1-50μm	System and resolution dependent, usually <10cm^3	Tabletop systems available, most systems stationary	>100,000	Radiation levels of <1μSv/h at scanner surface	3D, high resolution, quantitative analysis	Sample preparation time	Ritman 2004
OPT	1) Postmortem 2) Acquisition: 30-120 min Analysis: 2-20 min	Overall anatomical imaging, patterns of gene expression of whole embryos or whole organs	1-25 μm	System and resolution dependent, usually 1cm^3	Tabletop size and portable	>100,000	Avoid skin contact with clearing agent	3D, molecular specificity, high resolution	Specimen coverage	Sharpe et al. 2002 Sharpe 2004
UBM	1) In vivo 2) Acquisition: 15-45 min Analysis: 20-30 min	Most internal organs	~ 50 μm	Limited by depth of penetration through tissue (~1cm)	150 x 70 x 70 cm, Movable rolling cart	~250,000	None	Real time images up to 100 frames/sec, contrast agents available	Imaging depth of penetration, Poor tissue contrast	Foster et al 2000, 2002 Zhou et al. 2002
	UBM Mode	**Applications**								
	B-mode	General imaging of most internal organs (e.g., liver, heart, kidney, brain, placenta)								
	M-mode	Linear dimensions and motion over time of cardiovascular structures (e.g., heart, blood vessels)								
	Doppler	Blood flow velocities > 1 mm/sec (e.g., aorta, pulmonary artery, vena cava, atrioventricular junction, umbilical vessels)								

[a]3D, three-dimensional; MRI, magnetic resonance imaging; SEM, scanning electron microscopy; micro-CT, microcomputed tomography; OPT, optical projection tomography; UBM, ultrasound biomicroscope

1997). Injectable anesthetics (e.g., ketamine and pentobarbital) are not as safe or effective as inhalation anesthetics or hypothermia in newborn rodents (Danneman and Mandrell 1997).

The efficacy of euthanasia techniques also differs between mouse embryos and newborns and adult mice. The best form of euthanasia is one that occurs with minimal stress and pain. Pain perception in mouse embryos up to gestation day 15 is considered unlikely because cerebral cortical and subcortical neural development is minimal. Embryos up to gestational day 15 are nonviable so they can be euthanized humanely by euthanizing the pregnant mother and removing the embryos. After embryonic day 15, when embryos become viable and neural development advances to the stage where pain perception occurs, removed embryos can be euthanized by decapitation, cervical dislocation, carbon dioxide asphyxiation, or anesthesia followed by rapid freezing or fixation (http://oacu.od.nih.gov/ARAC/euthmous.pdf).

In pregnant mice, we induce isoflurane anesthesia in a chamber supplied with 5% isoflurane in oxygen. Anesthesia is maintained using a face mask supplied with 1 to 2% isoflurane in oxygen (i.e., the minimum concentration required to suppress spontaneous body movements). We monitor maternal body temperature using a rectal thermometer and maintain it between 36 and 38°C using a heating pad and lamp. Maintenance of appropriate maternal body temperature (e.g., see Table 2) and ventilation and oxygenation (Tobita et al. 2002) is critically important for maintaining normal maternal and embryonic cardiovascular function. The same procedure is used for newborns, except that we induce anesthesia by holding the newborn's face in the anesthetic mask supplied with 5% isoflurane. We monitor body temperature using a rectal probe in newborns more than 14 days of age, but not in younger mice because even though smaller probes are available, it is difficult to insert them safely. We use the same heat and anesthetic conditions for the younger and older newborns.

Single or repeated exposure to anesthesia may have long-term effects on embryonic and newborn mice, but these effects have not been studied in detail. It has been reported that chronic exposure to light isoflurane anesthesia (4 hr/day daily from embryonic days 6-15) reduced embryonic growth and increased the incidence of cleft palate (Mazze et al. 1985); however, the effect of repeated exposure to deeper levels of anesthesia is largely unexplored. We observed minimal effects on newborn mouse growth and cardiac diastolic function after repeated ultrasound examinations under isoflurane anesthesia (Zhou et al. 2003). Nevertheless, anesthesia and/or procedures (e.g., ultrasound or MRI) may affect physiological development, so appropriate controls are necessary.

Experimental Design and Statistical Considerations

Labeling Newborns for Longitudinal Studies

A major advantage of noninvasive in vivo phenotyping techniques such as ultrasound and MRI is that longitudinal studies can be performed in the same animal. A longitudinal study design reduces the number of animals required by allowing the same animal to contribute to multiple time points, reduces variability in the data so that fewer animals are required to achieve statistical significance, and, in cases where a phenotype has incomplete penetrance, it allows progression or regression of the phenotype to be studied in affected individuals. A requirement of longitudinal studies is the ability to identify individual animals and their contributions to the study data.

Newborns can be labeled on a short-term basis using permanent marker. The label must be refreshed daily. Tattooing provides a longer lasting label (Iwaki et al. 1989). We tattoo newborns on the bottom of the paw so the mark is still readily visible after the hair grows in (Figure 3). This procedure is performed by holding the newborn in one hand with the paw extended between the thumb and forefinger,

Table 2 Effect of maternal body temperature on embryonic cardiovascular function on day 17.5 of gestation (mean ± standard deviation)[a]

	No. of embryos	Normal 36.5-37.5°C	Low 34.5-35.0°C	*p* value
HR (bpm)	11	228 ± 36	167 ± 31	<0.001
ICT (ms)	11	25.6 ± 5	48.2 ± 12	<0.001
IRT (ms)	11	31.8 ± 3.9	48.1 ± 5.5	<0.001
ET (ms)	11	111 ± 16	142 ± 22	0.001
Tei index	11	0.52 ± 0.05	0.68 ± 0.04	<0.001
%FS	5	57.7 ± 3.6	46.2 ± 6.5	0.009

[a]HR, heart rate; ICT, isovolumic contraction time; IRT, isovolumic relaxation time; ET, ejection time, %FS, fractional shortening. Tei index (Myocardial Performance Index) is an index of global myocardial function (Broberg et al. 2003). Tei index = ((IRT + ICT)/ET).
All cardiac parameters in the embryos were significantly altered in mothers exposed to the lower temperature.

Figure 3 Tattoo markings on the paws of a newborn mouse.

and then placing an empty 29-gauge needle coated with india ink (a nontoxic suspension of carbon particles) onto the paw. The needle is inserted into the superficial layer of the skin and is advanced parallel to the skin surface along the length of the paw (Figure 3). Newborns can be uniquely identified by tattooing a combination of the four paws. Tattooing lasts for a minimum of 4 wk. At this stage mice are weaned, and ear clipping can be used for subsequent identification. Ideally, embryos studied in utero should be "tattooed" so they can be identified after birth. In future, it may be possible to accomplish this goal by using ultrasound-guided injections.

Inter- and Intralitter Variability

When determining the number of embryos or newborns to study, it is important to consider the degree of variability within and between litters. Even when different litters are identical genetically, variability within a litter may be considerably less than between litters. Therefore in terms of generalizing results to an entire population, N = 10 from one litter is not as useful as N = 1 from 10 litters. Developmental stages may differ by up to 1 day (Thiel et al. 1993) within a litter, possibly due to differences in the timing of fertilization. A more precise determination of gestational age can be achieved by staging embryos based on their morphological development (e.g., number of somites) (Papaioannou and Behringer 2005) or by size using ultrasound (Chang et al. 2003). Other factors that contribute to interlitter variability include differences in maternal physiology during pregnancy and maternal care of newborns. For example, we found that the coefficient of variation in newborn body weight was 5% within litters and 14% between litters on the day of birth (based on 60 newborns from 11 litters). A similar significant two-fold increase in variation was observed between litters for heart rate and an index of global myocardial function called the myocardial performance index (Broberg et al. 2003), whereas between- and within-litter variation did not differ significantly for other cardiovascular variables tested. Thus, if the goal is to generalize the results to the entire population, it is more efficient to study a subset of embryos or newborns from many litters. As a rule of thumb, we study one to four embryos or newborns from at least three, and usually five or more, litters.

Appropriate Controls

Choosing appropriate controls for the mutant can be problematic because many mutants are a hybrid of two or more strains, and large strain-dependent differences often exist in phenotypes (e.g., Mouse Phenome Database at The Jackson Laboratory, www.jax.org/phenome). Ideally, the only genetic difference between the mutant and control animals would be the targeted locus or transgene, but some compromises are usually necessary, as discussed in the literature (Sigmund 2000). This issue is also important when studying embryos and newborns because of the large differences in maternal body weight, embryo weight, and placental weight between strains, as illustrated in Figure 2.

Gestational and Postnatal Ages

In our laboratory, females are considered to be at day 0.5 of gestation at noon on the day a copulation plug is found in the vagina. However, the presence of a plug means that mating has occurred, not that the mouse is pregnant. The first indication of pregnancy may be an increasing maternal body weight. In ICR mice, successful pregnancy is detectable by ~day 4.5 of gestation, whereas it takes longer to detect pregnancy in the C57Bl/6J strain by monitoring maternal weight gain (Figure 2A). Uterine implantation sites can usually be detected by palpating the maternal abdomen by ~day 10.5. In our laboratory, we consider newborn mice to have a postnatal age of 0 day on the day of birth.

Phenotyping Methods for Use in Embryonic and Newborn Mice

Injection and Blood Sampling of Embryonic and Newborn Mice

A method for percutaneous injection of newborn mice between 0 and 4 days of age has been described (Sands and Barker 1999). Volumes up to 100 μL can be injected into the superficial temporal vein at this stage. In embryos at 6.5 days of gestation or older, microinjection of labeled cells or other agents into tissues or cavities of the embryo or placenta has been performed through the exteriorized uterus under image guidance by ultrasound (Slevin et al. 2006; Liu

et al. 1998) or transillumination, or based on visible extrauterine or transuterine landmarks (Mitchell et al. 2000; Papaioannou 1990). We have found that intravascular microinjection into the cardiac ventricles or large hepatic veins is possible in embryos ages 12.5 to 14.5 days using an ultrasound biomicroscope (UBM[1]) (Vevo660; VisualSonics, Toronto, Ontario, Canada) for image guidance (Slevin et al. 2006). Embryonic survival after cardiac microinjection of cells averaged 56% (85 of 115 injected embryos from 18 litters were alive when assessed 3 days after injection). This procedure can also be used to administer intracardiac microinjections of ~250 nL of india ink (Figure 4). Nagy and coauthors (2003) have reported using india ink to visualize the mouse embryonic vasculature by injecting into the vitelline vein of the yolk sac of embryo day 12.5 or older with aid of a mouth pipette. It is possible to inject ink with ultrasound guidance into the embryonic (days 12.5 to 14.5) left ventricle through a pulled-glass pipette (tip outer diameter <100 μm) at 23 nL/sec using a microinjector pump. After allowing the embryonic circulation to continue for several minutes to distribute the ink, the whole embryo was excised and immersed in fixative overnight before it was dehydrated through graded methanol solutions (25%-100%). Tissues were then cleared with a benzyl alcohol and benzyl benzoate 1:2 mixture to allow for three-dimensional (3D[1]) visualization of the vasculature (Figure 4).

Small volumes of blood may be collected from anesthetized newborns by cardiac puncture, and it may be possible to collect small volumes from the superficial temporal vein (Sands and Barker 1999). Larger volumes of blood can be obtained from the trunk after decapitation of newborns. As an example, ~40 μL (range 30-50 μL) was obtained by this method from ICR mouse newborns at 1 day postnatal age (body weight ~1.5 g). Embryonic blood can be obtained after cesarean delivery from the umbilical cord, by cardiac puncture, or after decapitation. Because we have found that it is possible to microinject into the heart of embryos under ultrasound guidance, it may also be possible to collect small volumes of blood via this route especially near the end of gestation, when embryos are relatively large.

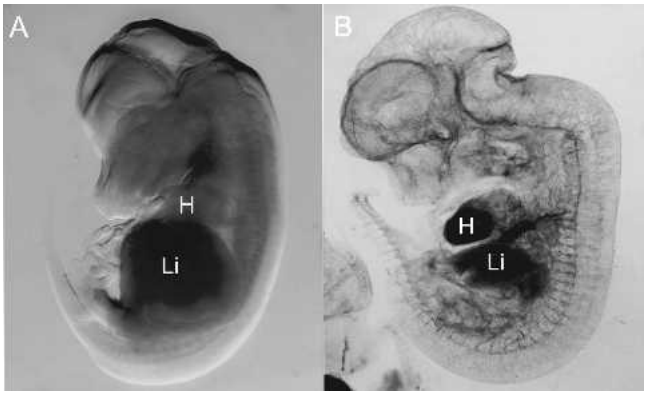

Figure 4 Vascular visualization of whole mount embryo after an in vivo intracardiac microinjection of india ink. (A) Control embryo at day 13.5; vasculature is poorly seen without ink. (B) Day 13.5 embryo after left ventricular microinjection of india ink in utero under ultrasound guidance. The ink has been distributed throughout the embryonic vascular system. Embryo tissues were cleared with a benzyl alcohol:benzyl benzoate mixture. H, heart; Li, liver.

Electrocardiography, Blood Pressure, and Heart Rate

We record ECG signals from isoflurane-anesthetized neonatal mice using copper tape to connect their paws to transcutaneous electrodes designed for adult mice (Indus Instruments, Houston, TX). Others report methods for recording ECG in awake newborn mice in specially designed chambers from 1 to 14 days postnatal age (Wang et al. 2000).

It is difficult to measure blood pressure in newborn mice. Tail cuff blood pressure systems cannot be used in mice before weaning because their tails are too short. It is also difficult to obtain high-fidelity arterial pressures using vascular catheters due to the relatively poor frequency response of such small diameter catheters (e.g., internal diameter of carotid artery is ~250 μm in 3- to 7-day-old newborns) and due to the capacitance of standard strain gauge transducers, which is high relative to the low blood volume in newborn mice. However, it is possible to measure blood pressure invasively in mouse embryos (Ishiwata et al. 2003) and in anesthetized newborn mice as young as the day of birth (Ishii et al. 2001) using a pulled-glass pipette and servo-null pressure recording system. ECG may not have been successfully measured in embryonic mice due to the difficulty in maintaining hemodynamic stability in exposed embryos as well as difficulties caused by size and low signal to noise ratios.

Doppler Ultrasound

Doppler instruments measure blood velocity by detecting the Doppler frequency shift in the signal reflected from moving red blood cells. Doppler signals can be used to assess systolic and diastolic cardiac function, to calculate vascular blood flow using vessel area, and to detect valvular defects, stenosis, and abnormalities in upstream or downstream vascular resistance. We measured intraventricular Doppler blood velocity waveforms in the left ventricle of postnatal mice from the day of birth in a study investigating diastolic function (Zhou et al. 2003). While performing this study, we found that strong Doppler signals could be readily obtained from the heart and from other vessels as early as the day of birth. As in adult mice (Hartley et al. 2002), this method provides a relatively inexpensive and effective tool for noninvasive phenotyping of cardiovascular function in newborns. However, skill and practice are required because

the Doppler sample volume must be placed without the benefit of a two-dimensional (2D[1]) ultrasound image for guidance. In embryos visualized after surgical exposure, Doppler ultrasound has been used to evaluate cardiac function in association with simultaneous measurements of cardiac dimensions using videomicroscopy (Keller et al. 1996).

Ultrasound Systems

Ultrasound systems can be used to obtain noninvasive real-time images from which one can obtain quantitative measurements of dimensions and assess areas and structural morphology. The image is also useful for placing the Doppler sample volume within vessels or the heart to obtain blood velocity information and for placing the "M-mode" cursor over the heart to obtain information on the motion and dimensions of the cardiac chambers over time. While clinical ultrasound systems have been used to phenotype embryonic and newborn mice, recent advances in ultrasound technology have led to the development of the UBM designed specifically for high-resolution imaging of mice (Foster et al. 2000, 2002).

Clinical ultrasound systems with relatively high-frequency transducers (~15 MHz) have been used to measure the size of the decidual sac from 7.5 days to obtain a noninvasive estimate of gestational age (Chang et al. 2003) and to measure embryonic size from 12.5 days to assist in phenotypic characterization (Leatherbury et al. 2003). Using this instrumentation, Doppler signals can also be obtained from the embryonic heart from ~12.5 days of gestation (Gui et al. 1996; Leatherbury et al. 2003) and M-mode recordings for evaluation of cardiac function from ~15.5 days (Leatherbury et al. 2003). However, the resolution of images generated using clinical ultrasound systems is poor (200-500 μm) compared with the resolution (~50 μm) of images using much higher frequency transducers (~40 MHz) of the UBM (Zhou et al. 2002). Indeed, the UBM can be used to measure the gestational sac from day 6.5 (Figure 5A) and to obtain Doppler measurements from embryos as soon as the heart begins to beat on day 8.5 of gestation (Figure 5, B and C) (Ji et al. 2003). Furthermore,

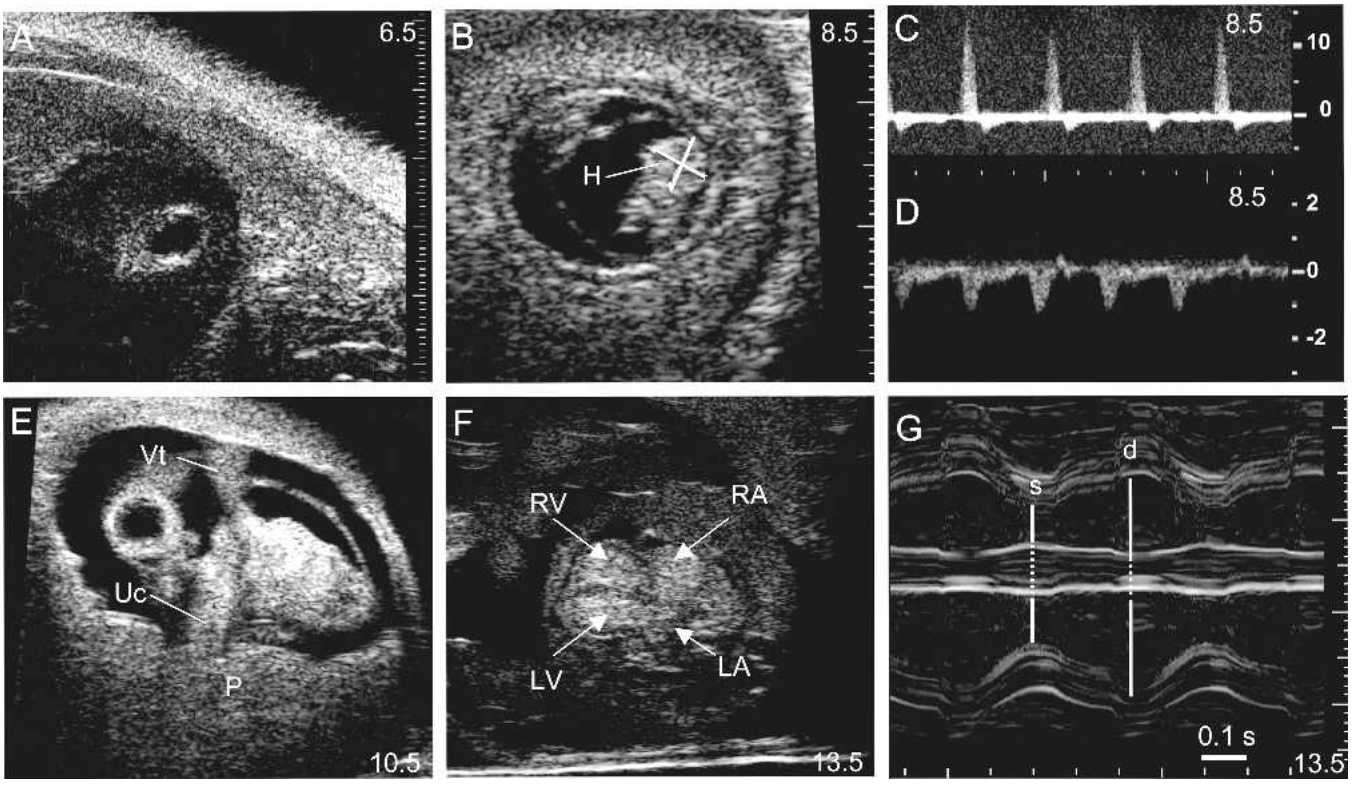

Figure 5 Ultrasound biomicroscope images, and Doppler and M-mode recordings from mouse embryos at various gestational ages. (A) Mouse embryo at 6.5 day of gestation (~2 days after implantation). Implantation sites are visible. (B) At day 8.5, cardiac size can be quantified by measuring the maximal width and length of the embryonic heart. (C) Flow velocity in the cardiac region is first detectable at day 8.5. Doppler waveforms can be used to quantify embryonic heart rate and detect arrhythmias. (D) Blood flow velocity in the vitelline circulation to the yolk sac is also first detectable at day 8.5. (E) At day 10.5, the vitelline artery and the umbilical cord are clearly visible. (F) At day 13.5, the four-chamber view of both ventricles and both atria can be obtained. (G) M-mode recording of embryo heart at day 13.5. H, heart; Vt, vitelline artery; Uc, umbilical cord; LA, left atrium; RA, right atrium; LV, left ventricle; P, placenta; RV, right ventricle; d, diastole; s, systole. Smallest units on scale bars in A, B, and G are 100 μm. Scale bars in C and D are in cm/sec.

the higher image resolution and smaller Doppler sample volume allow for more precise placement of the sample volume. The ability of this instrumentation to detect low blood velocities is important when studying low blood velocities in the embryonic circulation (Phoon et al. 2000; Zhou et al. 2002).

We have found that the age of lethality can be estimated using UBM B-mode imaging by determining the number of viable and nonviable implantation sites visible within the uterus as a function of gestational age. The absence of a heartbeat can be used to detect nonviable embryos on or after day 8.5 of gestation (Figure 5, B and C). However, an echolucent gestational sac surrounded by a relatively echobright region of trophoblast cells is visible by day 6.5 (Figure 5A). Size can be quantified using the UBM calipers. Implantation sites that are abnormally small with abnormal morphology contain nonviable resorbing embryos in our experience (23 of 23 abnormal sites contained nonviable embryos when examined between day 10.5 and 18.5 of gestation). It is important to note that some embryos may be missed when viewing with any ultrasound system, and this problem is particularly common when litter size is large. For example, when we compared the number of viable and nonviable embryos determined using the UBM with the number determined the same day by dissection, we found that we had missed 11% (23/262) of the live embryos and 21% (6/29) of the dead or resorbing embryos using the UBM. In this study, the mean litter size was seven (range 1-12) and the mean number of mice examined per day from 10.5 to 18.5 days was three (range 1-6). It is also important to note that with the exception of the embryos adjacent to the cervical attachment of the uterus, the same embryo may not be imaged on subsequent days even when found in the same intra-abdominal position because of the mobility of the uterine horns during pregnancy.

The UBM has been used for morphological, functional, and hemodynamic phenotyping of embryonic and newborn mice (Fatkin et al. 1999; Foster et al. 2003; Ji et al. 2003; Lickert et al. 2004; Phoon and Turnbull 2003; Phoon et al. 2000, 2004; Zhou et al. 2002, 2003). The amount of detailed phenotypic information that can be obtained by UBM imaging increases as gestation advances. In our experience, at day 6.5 of gestation (~2 days after implantation), the size of the implantation site can be quantified using calipers (Fig-

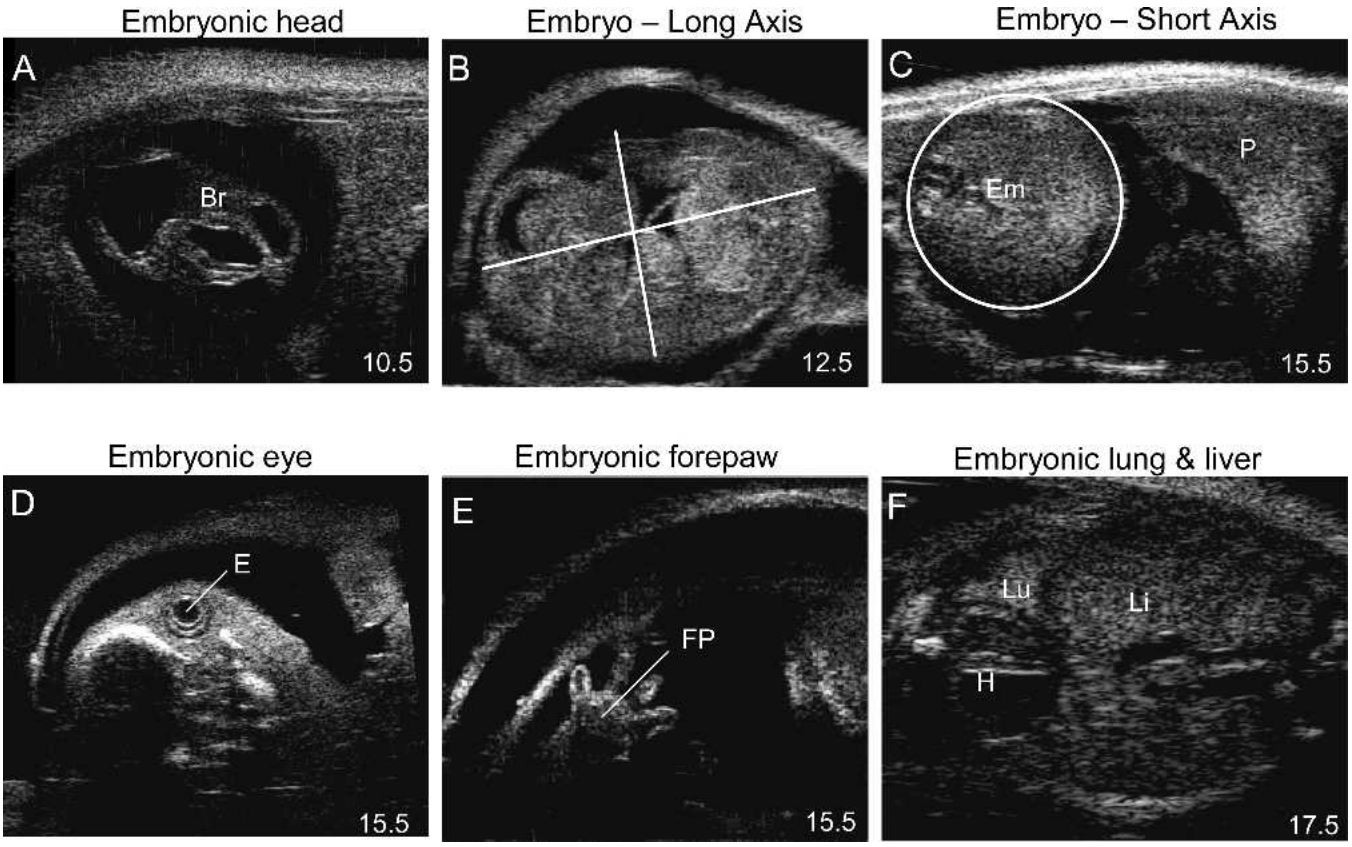

Figure 6 Embryonic structures visualized by ultrasound biomicroscope from day 10.5 to 17.5 of gestation. (A) Axial view of the embryonic head at day 10.5 showing the cerebral ventricles in the brain. (B) Long-axis view can be used to quantify embryo size by measuring the maximal width and length of the embryo. (C) Short-axis view can be used to quantify embryo size by determining the area of the embryo. B-mode images of embryonic eye (D), forepaw (E), liver and lung (F). Br, brain; P, placenta; Em, embryo; E, eye; FP, forepaw; Lu, lung; Li, liver; H, heart.

ure 5A). By day 8.5, when the embryonic heart has started to beat, it is possible to use Doppler to measure heart rate and to detect arrhythmias, and to use calipers to measure cardiac size (Figure 5, B and C). Blood flow velocity in the vitelline circulation to the yolk sac is also first detected at this stage (Figure 5D). By day 9.5, the umbilical circulation has formed (Figure 5E), and Doppler arterial waveforms can be obtained from the umbilical artery (Phoon et al. 2000) and from the inflow or outflow tracts of the heart (Zhou et al. 2002). Calipers can be used to measure embryonic size and cross-sectional area (e.g., Figure 6, B and C). By day 13.5 of gestation, when embryos are in a suitable orientation to obtain a four-chamber view of both ventricles and both atria (Figure 5F), the pulsed Doppler sample volume can be placed within the left or right ventricular chamber to record the mitral or tricupsid inflow, or within the ascending aorta to record the outflow blood velocity waveforms (e.g., Figure 7). By 13.5 days of gestation, when embryos are in a

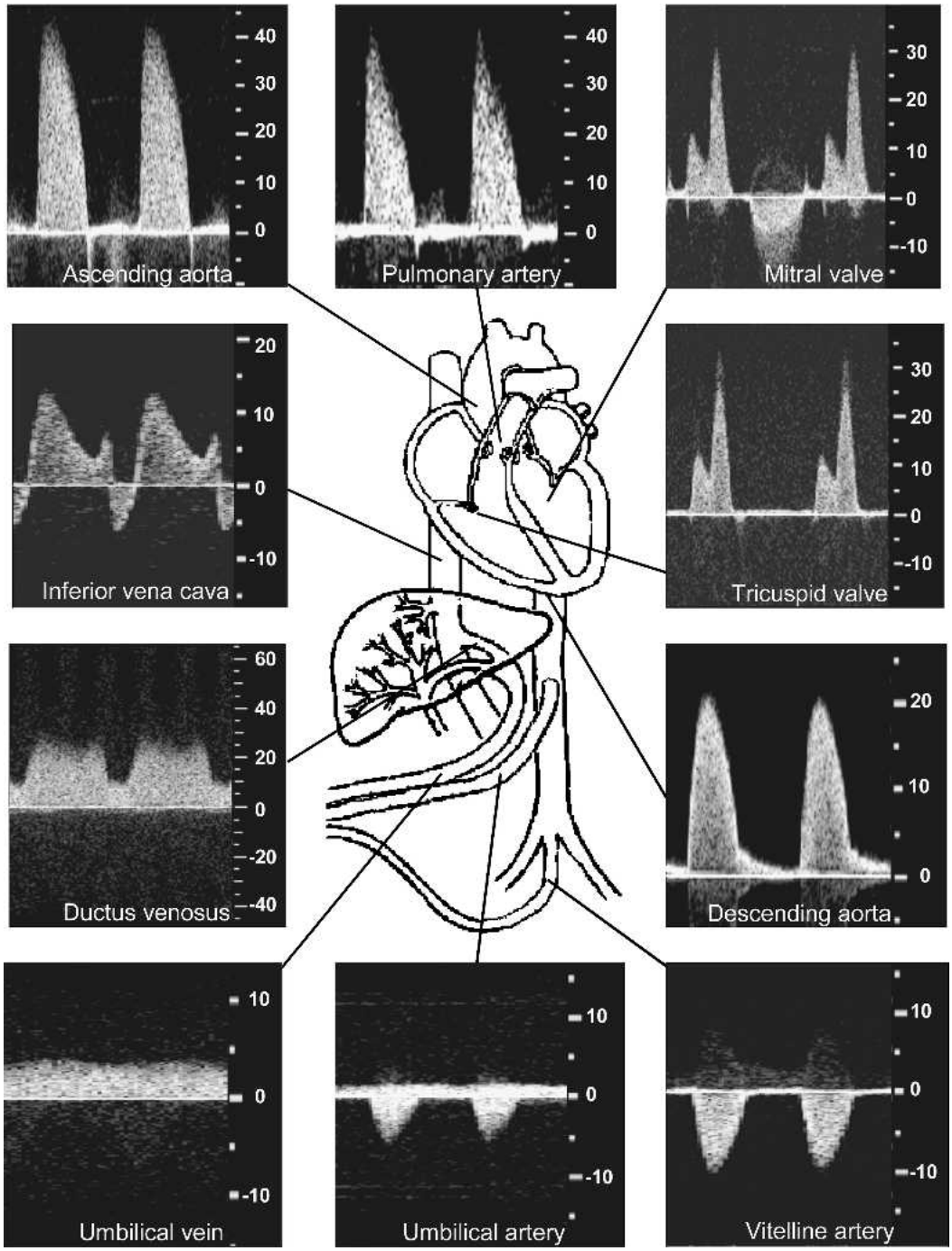

Figure 7 Doppler blood velocity waveforms obtained at various sites in the embryonic circulation. Scale bars in cm/sec.

suitable orientation to obtain a long-axis view of the left and right ventricles, it is possible to obtain M-mode recordings of the motion of the heart walls, in addition to the intraventricular waveforms (e.g., Figure 5G). Additionally, other structures can be examined for phenotypic analyses, including the brain, eyes, paws, lungs, and liver (Figure 6, A and D-F). Eye morphogenesis has been studied in vivo during development using this method (Foster et al. 2003). Doppler waveforms can also be obtained at other sites such as the ascending and descending aorta, the pulmonary artery, the umbilical and vitelline arteries, and the umbilical vein, ductus venosus, and inferior vena cava (Figure 7).

Using the methods described above, we have detected a variety of mutant phenotypes, including arrhythmia, abnormal umbilical arterial velocity waveforms (unpublished) similar to those observed in pathological human pregnancies (Harman and Baschat 2003), and abnormal kidney development (Figure 8). The UBM can be used to obtain similar information in newborn mice. Imaging tends to be easier in postnatal animals because the operator has more freedom to adjust body position and transducer angle to obtain the best imaging plane.

The bioeffects of diagnostic levels of ultrasound on mouse embryonic development appear to be modest or nonexistent after a single exposure although small transient reductions in postnatal body weight have been observed (Brown et al. 2004; Hande and Devi 1993). Pending further information on bioeffects, we limit each ultrasound examination to 60 min per pregnant mouse or newborn (from the onset of anesthesia to arousal), and we limit the number of ultrasound sessions in longitudinal studies to a maximum of five.

Magnetic Resonance Imaging

MRI detects the oscillations of nuclei whose spins produce a net magnetic moment in the presence of a strong magnetic field (Chatham and Blackband 2001). The most commonly imaged nucleus is the proton in water, which has magnetic

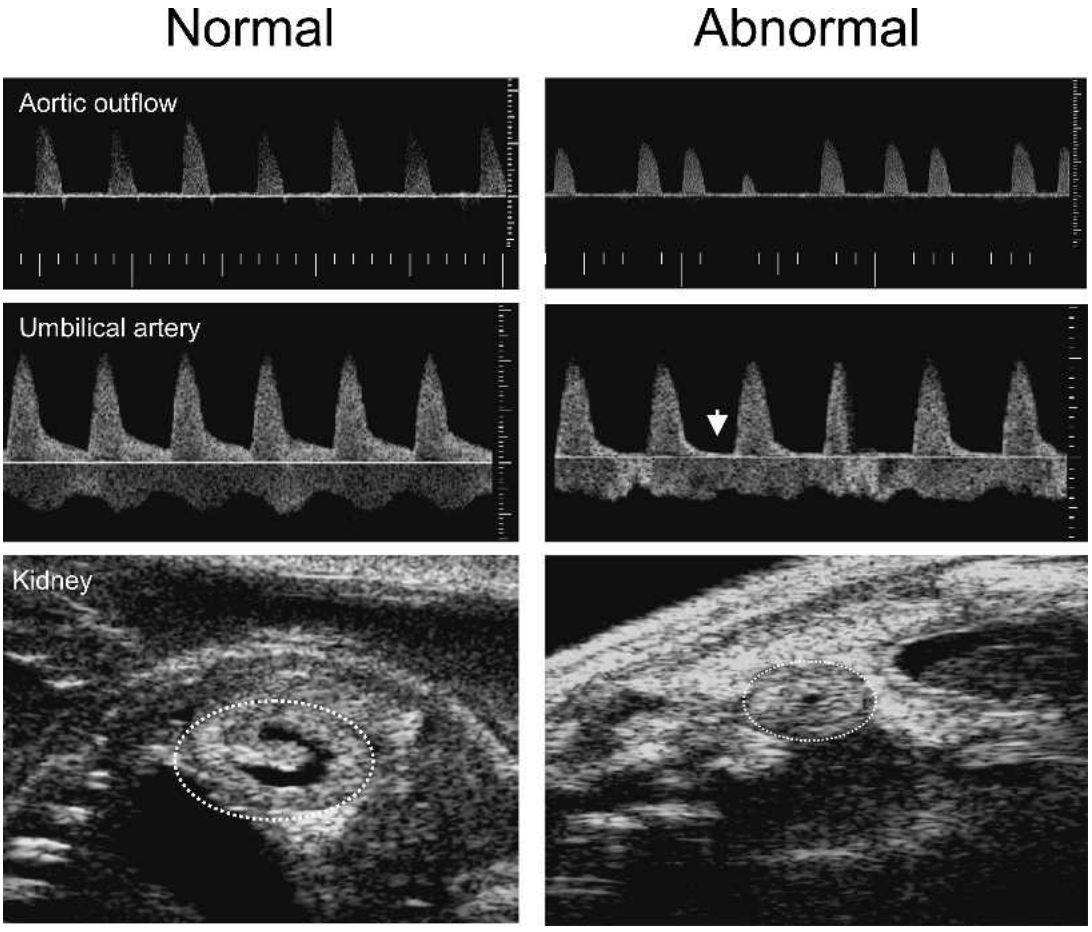

Figure 8 Normal and abnormal Doppler blood velocity waveforms, and kidneys in embryos. Arrhythmia was detected in the aortic velocity waveform from an embryo at 13.5 days of gestation (top). Abnormally low end-diastolic velocity (arrow) was detected in the umbilical arterial waveform from an embryo at 17.5 days of gestation (middle). Abnormally small kidneys were observed in an embryo at 17.5 days of gestation (bottom).

resonance properties that depend on its chemical environment and which provides good soft tissue contrast in images. MRI is advantageous for in vivo phenotyping because it presents realistic 3D anatomy without the shrinkage and distortion inherent in 2D serial histological sections.

Recent advances in MRI technology have increased image resolution approximately 10-fold so that it is now possible to obtain images in mice with a diagnostic quality similar to that obtained in humans using clinical MRI systems. This result has been achieved by using more powerful magnets (~5-12 tesla) than are typically used in clinical MRI systems (~1.5-3.0 tesla) and by using much smaller radiofrequency coils, thereby greatly increasing sensitivity. It is also possible to use long imaging times to increase image resolution. MRI can be used to image the entire newborn with an isotropic resolution of 100 μm. Because the tissue contrast is also similar to that of human MRI, translational studies are possible with mouse models of disease (Nieman et al. 2005). However, to probe the underlying cytoarchitecture, histology is still needed because MRI lacks the fidelity to resolve detail at the cellular level.

In Figure 9, an example of an MRI image of the head region of a live 6-day-old mouse newborn is shown. The mouse was given Mn^{2+} as a contrast agent (Watanabe et al. 2004), and the resolution of the 3D image is 100 μm isotropic. The image reveals good detail for analyzing gross brain anatomy. Despite the fact that it takes 3 hr to produce such an image, which is a drawback in MRI, multiple-mouse MRI can considerably increase the throughput in a study (Bock et al. 2003). MRI is also sensitive to motion, so gating techniques (Cassidy et al. 2004) are needed when imaging near the heart and lungs in newborns. Motion artifacts are problematic when imaging mouse embryos in vivo, although some progress has been made (e.g., Hogers et al. 2000). Thus embryos are usually imaged postmortem and after fixation (Smith 2000). Gadolinium contrast agents may be infused to enhance visualization of the cardiovascular system (Smith 2000). Postmortem imaging enables isotropic image resolutions of up to 25 μm (Schneider et al. 2003) by eliminating motion artifacts and by permitting much longer imaging times.

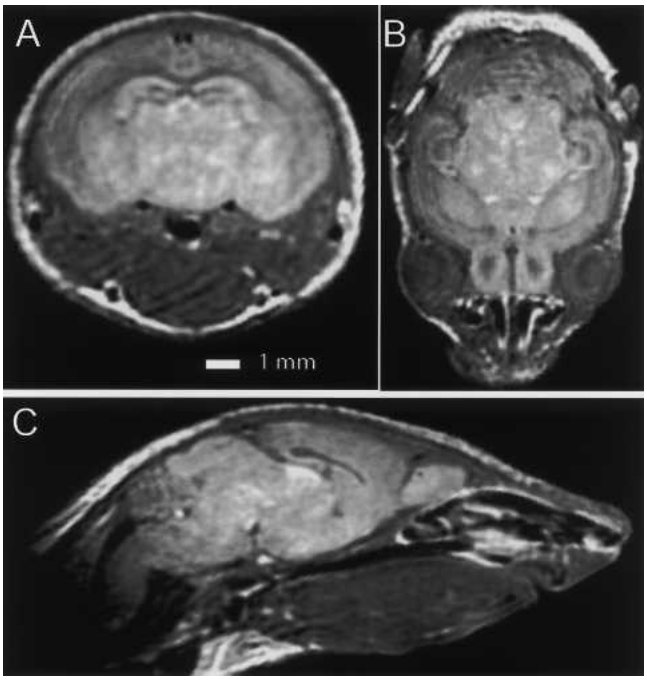

Figure 9 Magnetic resonance images of a live 6-day-old mouse pup showing three orthogonal slices—(A) coronal, (B) horizontal, and (C) sagittal—obtained from a three-dimensional (3D) image of the skull and brain. The mouse was given Mn^{2+} as a contrast agent. The resolution of the 3D image was 100 μm isotropic. The image shows good detail for analyzing gross brain anatomy.

Vascular Corrosion Casting

Vascular corrosion casting is an acute invasive method that is available for investigating normal and abnormal vascular anatomy of the mouse embryonic and placental circulations. Plastic casts permit 3D visualization of the structure of the blood spaces. Casts are made by clearing the blood from the vessels of interest and then infusing a liquid plastic such as methyl methacrylate (Polysciences, Inc., Warrington, PA), which hardens within the vessels. To cast the uteroplacental vasculature, a catheter is placed in the descending thoracic aorta of the pregnant mouse, and the casting compound is infused into the lower body vasculature including the uterus and placentas. A fine-tipped glass cannula attached to a double-lumen catheter is used to instill the same casting compound into either the vessels of the embryonic side of the placenta or the embryonic circulation via the umbilical artery or vein. After polymerization of the casting compound, tissues are digested from the hardened casts using a concentrated base solution (20% KOH). The washed and dried casts are then available for light or scanning electron microscopy (SEM[1]) (Kondo 1998; Whiteley et al. 2006). This method has been used to cast the mouse uteroplacental vasculature from 5.5 to 18.5 days gestation, and the vasculature of the embryonic side of the placenta and embryonic vasculatures from 12.5 days gestation to term (Adamson et al. 2002; Kondo 1998) (Figure 10).

Vascular casts can provide both qualitative and quantitative information on vessel number and diameter. The blood spaces so obvious in vascular casts often collapse during tissue dissection and processing for histology, leaving them barely detectable on histological sections. In addition, casts provide information on the surface morphology of cells lining the blood-perfused spaces. This feature can be used to distinguish blood spaces that are lined by arterial or venous endothelial cells, or by trophoblast cells (Adamson et al. 2002). When viewed with an SEM, individual capillaries are visible in vascular corrosion casts (e.g., Figure 10A). Depending on their location within the cast, dissection or trimming of the plastic cast may be necessary to

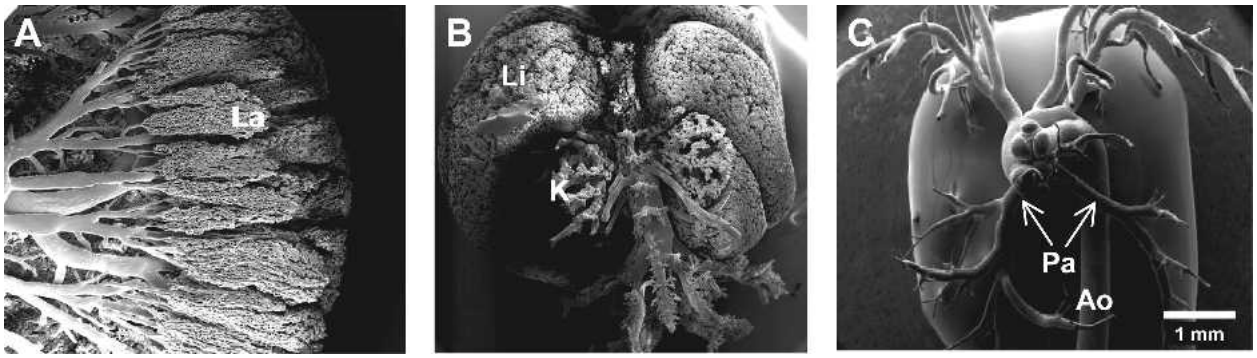

Figure 10 Vascular corrosion casts of the placental and embryonic circulations. (A) Image of a vascular corrosion cast of the embryonic side of the placental microcirculation at 17.5 days of gestation obtained using a scanning electron microscope (SEM). (B) Image of the venous circulation of a mouse embryo at 15.5 days of gestation obtained using a SEM. (C) Image of a cast showing the major arterial vasculature of a 17.5 day mouse embryo obtained using a SEM. Infusion of the casting compound was stopped before reaching the small arterioles and capillaries to prevent them from obscuring the view of the larger vessels. La, labyrinth; Li, liver; K, kidney; Pa, pulmonary arteries; Ao, descending aorta.

expose vessels of interest. Alternatively, partial filling of the embryonic (Figure 10C) or placental circulations (Adamson et al. 2002) from either the arterial or venous sides is possible.

Microcomputed Tomography

Microcomputed tomography (micro-CT[1]) (Ritman 2004), is a rapidly advancing X-ray technology stimulated by the recent demand for small animal imaging. Air, fatty tissue, nonfatty tissue, and bone can be distinguished in micro-CT images (Ritman 2004). Other spaces can be discerned by using X-ray contrast agents. To image the vasculature, contrast is obtained by perfusing the specimen with a radiopaque polymer that sets within the vascular space. Because the surrounding tissue is relatively transparent to X-rays, the tissue masceration required for other casting techniques is not needed when preparing a specimen for micro-CT. Moreover, the ability to produce 3D data sets affords more flexibility in visualization and analysis than light or electron microscopy. Tabletop micro-CT systems can resolve 20-μm diameters and larger vessels over a 2- to 3-cm field of view (Bentley et al. 2002; Marxen et al. 2004), and synchrotron-based systems have been demonstrated with 1-μm resolution (Heinzer et al. 2004), sufficient to resolve individual capillaries. Given the field of view, micro-CT is limited to studying vascular networks in individual organs in adult mice but can be used to visualize the entire vascular network of embryos and their placentas.

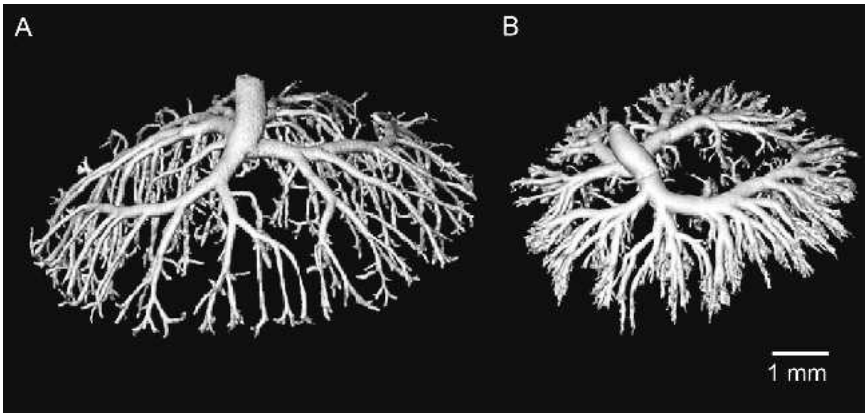

Figure 11 Microcomputed tomography (micro-CT) image of the embryonic side of the placental circulation at day 15.5 of gestation. The contrast agent was injected into (A) the umbilical artery until the capillaries started to fill to visualize the arterial side of the placental circulation, and into (B) the umbilical vein until the capillaries started to fill to visualize the venous side of the circulation. Micro-CT was unable to resolve individual capillaries, thus the capillary beds have not been included in these images. The absence of the capillaries permits an unobstructed view of the arterial and venous circulation. The voxel size for the reconstructed images was 13 μm.

To obtain the images shown in Figure 11, the arterial or venous circulations of the embryonic side of the placental circulation were perfused with Microfil (Flow Tech Inc., Carver, MA) contrast agent using the infusion method described in Vascular Corrosion Casting above. Specimens were scanned in an MS-9 micro-CT scanner (GE Medical Systems, London, Ontario) to produce data sets with a voxel size of 13 μm. Reconstruction produced 3D images and enabled generation of geometric models of the lumen surface, excluding capillaries. Lumen surface renderings are shown in Figure 11 for arterial and venous casts of the embryonic side of the placental circulation. Using computer-based analysis, geometric properties such as surface area and vessel diameter distributions can be derived (Rennie et al. 2005; Sled et al. 2004). Automation of these measurements facilitates population studies and the characterization of disease models.

Optical Projection Tomography

Optical projection tomography (OPT[1]), a new technique that is now commercially available (www.bioptonics.com), generates very high resolution images of clarified embryos or whole organs. It is essentially an optical version of micro-CT that uses image-forming optics and optical contrast agents to create cellular resolution 3D images of whole specimens up to 1 cubic centimeter in size (Sharpe 2004; Sharpe et al. 2002). In the OPT method, a specimen is embedded in agarose, clarified in a 1:2 solution of benzyl alcohol:benzyl benzoate, and then affixed to a rotating stage. The specimen is rotated stepwise through a complete revolution, and at each step an image is acquired using a microscope and a charge-coupled device camera. The images are used in a typical backprojection algorithm to reconstruct a 3D image of the complete specimen. The final result is a 3D data set that can be viewed in a slice-by-slice manner (Figure 12, B and C), or surface or volume rendered to obtain a true 3D representation of the data (Figure 12A).

OPT can be used in either transmission or fluorescent mode, which are similar to brightfield and fluorescence microscopy, respectively. Each mode can take advantage of the multitude of absorbing and fluorescent molecularly specific contrast agents that have been developed over many years of microscopy. Gene-specific markers can be used to study the pattern of gene expression throughout the entire specimen (Baldock et al. 2003) or to enhance visualization of a structure of interest (Lickert et al. 2004). Optical filters are used to separate the molecular marker signal from the autofluorescence signal in order to acquire two sets of images at each view angle, and thus two overlapping 3D OPT data sets. In this manner, the position of the pattern or structure with respect to the rest of the specimen is maintained. Mutant/wild-type comparisons performed with OPT (Lickert et al. 2004; von Both et al. 2004) are more sensitive to spatial complexity than comparisons performed using serial sectioning techniques that may alter subtle morphology.

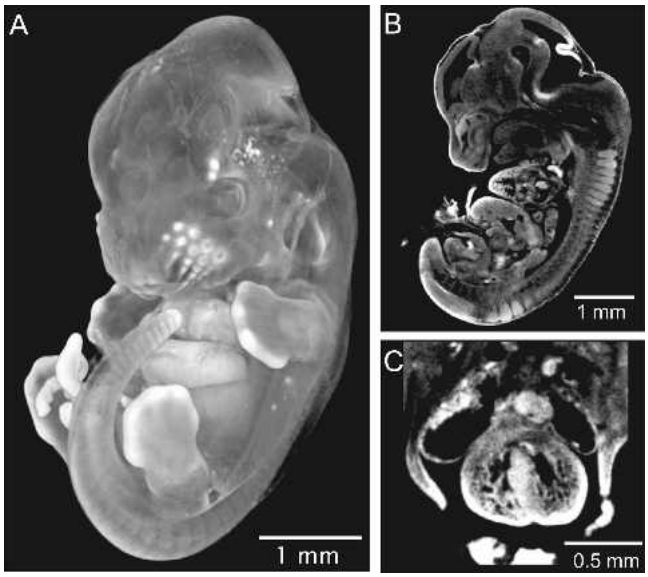

Figure 12 Optical projection tomography (OPT) image of a day 12.5 mouse embryo. (A) Volume rendering of an autofluorescence OPT data set. (B) Sagittal slice through the same embryo. (C) Axial section through the same embryo showing a zoomed image of the cardiac region. The voxel size for these OPT reconstructions was 16 μm.

OPT is ideally suited to morphological studies of whole mouse embryos of 8.5 to 15.5 days gestation or whole organs from older embryos or newborn mice.

Summary and Conclusion

Although the small size of mouse embryos and newborns presents a challenge, considerable progress has been made in adapting and miniaturizing technology to obtain increasingly detailed phenotypic information in embryonic and neonatal mice. The developmental stage of the animals being phenotyped is an important consideration when selecting the appropriate technique for anesthesia or euthanasia, and for labeling animals in longitudinal studies. It is also essential to maintain normal maternal cardiorespiratory state and body temperature before acquiring physiological data from embryos. In addition, it is important to control for possible study design differences between inter- and intralitter variability, and for possible long-term developmental effects caused by anesthesia and/or other procedures. Noninvasive or minimally invasive intravenous or intracardiac injections or blood sampling as well as arterial pressure and ECG measurements are feasible in newborns. Whereas microinjection techniques are available for embryos as young as 6.5 days of gestation, further development is required to obtain minimally invasive fluid or tissue samples, or blood pressure or ECG measurements, from mouse embryos in utero. Doppler and M-mode ultrasound can be used noninvasively to monitor cardiac and vascular hemodynamics in

vivo in embryos and newborns. In addition, sophisticated methods for imaging mouse embryos and newborns are available and include in vivo ultrasound and MRI, postmortem MRI, vascular corrosion casts, micro-CT, and OPT. This growing repertoire of techniques available for phenotyping mouse embryos and newborns is critical to gain maximal benefit from genetically engineered mice as models for advancing our understanding of the genesis of congenital diseases, and our knowledge of gene function during development.

Acknowledgments

This work was funded by operating and/or equipment grants from the Canadian Institutes of Health Research, the Canadian Foundation for Innovation, Ontario Innovation Trust, Ontario Research and Development Challenge Fund, National Cancer Institute of Canada, Burroughs Wellcome Fund, National Institutes of Health, and the Richard Ivey Foundation. S.L.A. is a member of the Scientific Advisory Board of the VisualSonics Company and has no financial interests in the company.

References

Adamson SL, Lu Y, Whiteley KJ, Holmyard D, Hemberger M, Pfarrer C, Cross JC. 2002. Interactions between trophoblast cells and the maternal and fetal circulation in the mouse placenta. Dev Biol 250:358-373.

Baldock RA, Bard JB, Burger A, Burton N, Christiansen J, Feng G, Hill B, Houghton D, Kaufman M, Rao J, Sharpe J, Ross A, Stevenson P, Venkataraman S, Waterhouse A, Yang Y, Davidson DR. 2003. EMAP and EMAGE: A framework for understanding spatially organized data. Neuroinformatics 1:309-325.

Bentley MD, Ortiz MC, Ritman EL, Romero JC. 2002. The use of microcomputed tomography to study microvasculature in small rodents. Am J Physiol Reg Integr Comp Physiol 282:R1267-R1279.

Bock NA, Konyer NB, Henkelman RM. 2003. Multiple-mouse MRI. Mag Res Med 49:158-167.

Broberg CS, Pantely GA, Barber BJ, Mack GK, Lee K, Thigpen T, Davis LE, Sahn D Hohimer AR. 2003. Validation of the myocardial performance index by echocardiography in mice: A noninvasive measure of left ventricular function. J Am Soc Echocardiogr 16:814-823.

Brown AS, Reid AD, Leamen L, Cucevic V, Foster FS. 2004. Biological effects of high-frequency ultrasound exposure during mouse organogenesis. Ultrasound Med Biol 30:1223-1232.

Bruneau BG. 2003. The developing heart and congenital heart defects: A make or break situation. Clin Genet 63:252-261.

Cassidy PJ, Schneider JE, Grieve SM, Lygate C, Neubauer S, Clarke K. 2004. Assessment of motion gating strategies for mouse magnetic resonance at high magnetic fields. J Mag Res Imaging 19:229-237.

Chang C-P, Chen L, Crabtree GR. 2003. Sonographic staging of the developmental status of mouse embryos in utero. Genesis 36:7-11.

Chatham JC, Blackband SJ. 2001. Nuclear magnetic resonance spectroscopy and imaging in animal research. ILAR J 42:189-208.

Conway SJ, Kruzynska-Frejtag A, Kneer PL, Machnicki M, Koushik SV. 2003. What cardiovascular defect does my prenatal mouse mutant have, and why? Genesis 35:1-21.

Copp AJ. 1995. Death before birth: Clues from gene knockouts and mutations. Trends Genet 11:87-93.

Danneman PJ, Mandrell TD. 1997. Evaluation of five agents/methods for anesthesia of neonatal rats. Lab Anim Sci 47:386-395.

Fatkin D, Christe ME, Aristizabal O, McConnell BK, Srinivasan S, Schoen FJ, Seidman CE, Turnbull DH, Seidman JG. 1999. Neonatal cardiomyopathy in mice homozygous for the Arg403Gln mutation in a cardiac myosin heavy chain gene. J Clin Invest 103:147-153.

Foster FS, Pavlin CJ, Harasiewicz KA, Christopher DA, Turnbull DH. 2000. Advances in ultrasound biomicroscopy. Ultrasound Med Biol 26:1-27.

Foster FS, Zhang M, Duckett AS, Cucevic V, Pavlin CJ. 2003. In vivo imaging of embryonic development in the mouse eye by ultrasound biomicroscopy. Invest Ophthalmol Vis Sci 44:2361-2366.

Foster FS, Zhang MY, Zhou YQ, Liu G, Mehi J, Cherin E, Harasiecwicz KA, Starkoski BG, Zan L, Knapik DA, Adamson SL. 2002. A new ultrasound instrument for in vivo microimaging of mice. Ultrasound Med Biol 28:1165-1172.

Furukawa S, MacLennan MJ, Keller BB. 1998. Hemodynamic response to anesthesia in pregnant and nonpregnant ICR mice. Lab Anim Sci 48: 357-363.

Gui Y-H, Linask KK, Khowsathit P, Huhta JC. 1996. Doppler echocardiography of normal and abnormal embryonic mouse heart. Pediatr Res 40:633-642.

Hande MP, Devi PU. 1993. Effect of in utero exposure to diagnostic ultrasound on the postnatal survival and growth of mouse. Teratology 48:405-411.

Harman CR, Baschat AA. 2003. Arterial and venous Dopplers in IUGR. Clin Obstet Gynecol 46:931-946.

Hartley CJ, Taffet GE, Reddy AK, Entman ML, Michael LH. 2002. Noninvasive cardiovascular phenotyping in mice. ILAR J 43:147-158.

Heinzer S, Krucker T, Stampanoni M, Abela R, Meyer EP, Schuler A, Schneider P, Muller R. 2004. Hierarchical bioimaging and quantification of vasculature in disease models using corrosion casts and microcomputed tomography. In: Bonse U, ed. Developments in X-Ray Tomography IV. Bellingham WA:The International Society for Optical Engineering (SPIE). p 65-76.

Hogers B, Gross D, Lehmann V, Zick K, De Groot HJM, Gittenberger-de Groot AC, Poelmann RE. 2000. Magnetic resonance microscopy of mouse embryos in utero. Anat Rec 260:373-377.

Ishii T, Kuwaki T, Masuda Y, Fukuda Y. 2001. Postnatal development of blood pressure and baroreflex in mice. Auton Neurosci 94:34-41.

Ishiwata T, Nakazawa M, Pu WT, Tevosian SG Izumo S. 2003. Developmental changes in ventricular diastolic function correlate with changes in ventricular myoarchitecture in normal mouse embryos. Circ Res 93:857-865.

Iwaki S, Matsuo A, Kast A. 1989. Identification of newborn rats by tattooing. Lab Anim 23:361-364.

Ji RP, Phoon CKL, Aristizábal O, McGrath KE, Palis J, Turnbull DH. 2003. Onset of cardiac function during early mouse embryogenesis coincides with entry of primitive erythroblasts into the embryo proper. Circ Res 92:133-135.

Jones EA, Baron MH, Fraser SE Dickinson ME. 2004. Measuring hemodynamic changes during mammalian development. Am J Physiol Heart Circ Physiol 287:H1561-H1569.

Jones EA, Crotty D, Kulesa PM, Waters CW, Baron MH, Fraser SE Dickinson ME. 2002. Dynamic in vivo imaging of postimplantation mammalian embryos using whole embryo culture. Genesis 34:228-235.

Keller BB, MacLennan MJ, Tinney JP Yoshigi M. 1996. In vivo assessment of embryonic cardiovascular dimensions and function in day-10.5 to -14.5 mouse embryos. Circ Res 79:247-255.

Kondo S. 1998. Microinjection methods for visualization of the vascular architecture of the mouse embryo for light and scanning electron microscopy. J Electron Microsc (Tokyo) 47:101-113.

Leatherbury L, Yu Q, Lo CW. 2003. Noninvasive phenotypic analysis of cardiovascular structure and function in fetal mice using ultrasound. Birth Defects Res Part C Embryo Today 69:83-91.

Lickert H, Takeuchi JK, von B, I, Walls JR, McAuliffe F, Adamson SL, Henkelman RM, Wrana JL, Rossant J, Bruneau BG. 2004. Baf60c is

essential for function of BAF chromatin remodelling complexes in heart development. Nature 432:107-112.

Liu A, Joyner AL, Turnbull DH. 1998. Alteration of limb and brain patterning in early mouse embryos by ultrasound-guided injection of Shh-expressing cells. Mech Dev 75:107-115.

Marxen M, Thornton MM, Chiarot CB, Klement G, Koprivnikar J, Sled JG, Henkelman RM. 2004. MicroCT scanner performance and considerations for vascular specimen imaging. Med Phys 31:305-313.

Mazze RI, Wilson AI, Rice SA, Baden JM. 1985. Fetal development in mice exposed to isoflurane. Teratology 32:339-345.

Mitchell M, Jerebtsova M, Batshaw ML, Newman K, Ye X. 2000. Long-term gene transfer to mouse fetuses with recombinant adenovirus and adeno-associated virus (AAV) vectors. Gene Ther 7:1986-1992.

Nagy A, Gertsenstein M, Vintersten K, Behringer R. 2003. Techniques for visualizing gene products, cells, tissues, and organ systems. In: Manipulating the Mouse Embryo. A Laboratory Manual. III. Cold Spring Harbor NY: Cold Spring Harbor Laboratory Press. p 702-703, Protocol 24.

Nakazawa M, Morishima M, Tomita H, Tomita SM, Kajio F. 1995. Hemodynamics and ventricular function in the day-12 rat embryo: Basic characteristics and the responses to cardiovascular drugs. Pediatr Res 37:117-123.

Nieman BJ, Bock NA, Bishop J, Chen XJ, Sled JG, Rossant J, Henkelman RM. 2005. Magnetic resonance imaging for detection and analysis of mouse phemotypes. NMR Biomed 18:447-468.

Papaioannou VE. 1990. In utero manipulation. In: Copp AJ, Cockroft DL, eds. Postimplantation Mammalian Embryos: A Practical Approach. New York:Oxford University Press. p 61-80.

Papaioannou VE, Behringer RR, eds. 2005. Mouse Phenotypes. A Handbook of Mutation Analysis. Cold Spring Harbor NY: Cold Spring Harbor Laboratory Press.

Phoon CKL, Aristizabal O, Turnbull DH. 2000. 40 MHz Doppler characterization of umbilical and dorsal aortic blood flow in the early mouse embryo. Ultrasound Med Biol 26:1275-1283.

Phoon CKL, Ji RP, Aristizábal O, Worrad DM, Zhou B, Baldwin HS, Turnbull DH. 2004. Embryonic heart failure in NFATc1-/- mice. Novel mechanistic insights from in utero ultrasound biomicroscopy. Circ Res 95:92-99.

Phoon CKL, Turnbull DH. 2003. Ultrasound biomicroscopy-Doppler in mouse cardiovascular development. Physiol Genomics 14:3-15.

Rennie MY, Whiteley KJ, Adamson SL, Sled JG. 2005. Quantification of murine fetoplacental vasculature using micro computed tomography. Placenta 26:A14.

Ritman EL. 2004. Micro-computed tomography—Current status and developments. Annu Rev Biomed Eng 6:185-208.

Sands MS, Barker JE. 1999. Percutaneous intravenous injection in neonatal mice. Lab Anim Sci 49:328-330.

Schneider JE, Bamforth SD, Farthing CR, Clarke K, Neubauer S, Bhattacharya S. 2003. High-resolution imaging of normal anatomy, and neural and adrenal malformations in mouse embryos using magnetic resonance microscopy. J Anat 202:239-247.

Sharpe J. 2004. Optical projection tomography. Annu Rev Biomed Eng 6:209-228.

Sharpe J, Ahlgren U, Perry P, Hill B, Ross A, Hecksher-Sorensen J, Baldock R, Davidson D. 2002. Optical projection tomography as a tool for 3D microscopy and gene expression studies. Science 296:541-545.

Sigmund CD. 2000. Viewpoint: Are studies in genetically altered mice out of control? Arterioscler Thromb Vasc Biol 20:1425-1429.

Sled JG, Marxen M, Henkelman RM. 2004. Analysis of micro-vasculature in whole kidney speciments using micro-CT. In: Bonse U, ed. Development in X-Ray Tomography IV. Bellingham WA: The International Society for Optical Engineering (SPIE). p 53-64.

Slevin J, Byers L, Gertsenstein M, Qu D, Mu J, Sunn N, Kingdom J, Rossant J, Adamson SL. 2006. High resolution ultrasound-guided microinjection for interventional studies of early embryonic and placental development in vivo in mice. BMC Dev Biol (In Press).

Smith BR. 2000. Magnetic resonance imaging analysis of embryos. Methods Mol Biol 135:211-216.

Stimpfel TM, Gershey EL. 1991. Selecting anesthetic agents for human safety and animal recovery surgery. FASEB J 5:2099-2104.

Tei C, Nishimura RA, Seward JB, Tajik AJ. 1997. Noninvasive Doppler-derived myocardial performance index: Correlation with simultaneous measurements of cardiac catheterization measurements. J Am Soc Echocardiogr 10:169-178.

Thiel R, Chahoud I, Jurgens M, Neubert D. 1993. Time-dependent differences in the development of somites of four different mouse strains. Teratog Carcinog Mutagen 13:247-257.

Tobita K, Tinney JP, Keller BB. 2002. Cardiovascular phenotype analysis of murine embryos. In: Hoit BD, Walsh RA, eds. Cardiovascular Physiology in the Genetically Engineered Mouse. 2nd Ed. New York: Kluwer Academic Publishers. p 353-376.

von Both I, Silvestri C, Erdemir T, Lickert H, Walls JR, Henkelman RM, Rossant J, Harvey RP, Attisano L, Wrana JL. 2004. Foxh1 is essential for development of the anterior heart field. Dev Cell 7:331-345.

Wagman AJ, Hu N, Clark EB. 1990. Effect of changes in circulating blood volume on cardiac output and arterial and ventricular blood pressure in the stage 18, 24, and 29 chick embryo. Circ Res 67:187-192.

Wang L, Swirp S, Duff H. 2000. Age-dependent response of the electrocardiogram to K+ channel blockers in mice. Am J Physiol Cell Physiol 278:C73-C80.

Watanabe T, Radulovic J, Spiess J, Natt O, Boretius S, Frahm J, Michaelis T. 2004. In vivo 3D MRI staining of the mouse hippocampal system using intracerebral injection of MnCl2. Neuroimage 22:860-867.

Whiteley KJ, Pfarrer C, Adamson SL. 2006. Vascular corrosion casting of the uteroplacental and fetoplacental vasculature in mice. In: Soares MJ, Hunt JS, eds. Methods in Molecular Medicine. Placenta and Trophoblast: Methods and Protocols. Totowa NJ: Humana Press 121:371-392.

Zhou YQ, Foster FS, Qu DW, Zhang M, Harasiewicz KA, Adamson SL. 2002. Applications for multifrequency ultrasound biomicroscopy in mice from implantation to adulthood. Physiol Genomics 10:113-126.

Zhou Y-Q, Foster FS, Parkes R, Adamson SL. 2003. Developmental changes in left and right ventricular diastolic filling patterns in mice. Am J Physiol Heart Circ Physiol 285:H1563-H1575.